Inorg. Chem. **2006**, *45*, 4951–4962

Equilibria and Structure of the Lanthanide(III)-2-hydroxy-1,3-diaminopropane-*N*,*N*,*N*′,*N*′-tetraacetate Complexes: Formation of Alkoxo-Bridged Dimers in Solid State and Solution

Gyula Tircsó,*,‡,§ Attila Bényei,† Ernõ Brücher,*,‡ Anita Kis,‡ and Róbert Király‡

Department of Chemistry, Laboratory for X-ray Diffraction, Department of Inorganic and Analytical Chemistry, University of Debrecen, Egyetem tér 1, Debrecen H-4010, Hungary

Received October 6, 2005

The complex formed between 1,3-diamino-2-hydroxypropane-*N*,*N*,*N*′,*N*′-tetraacetic acid (H_4L-OH) and Nd^{3+} at pH 7.5 was found to be a dinuclear dimer in the solid state by X-ray crystallography. In the complex $K_4[Nd_2(L\text{-}O)_2(H_2O)_2]\cdot 14H_2O$ each ligand is coordinated to both Nd^{3+} atoms with an iminodiacetate group (the Nd^{3+}–Nd^{3+} distance is 3.9283(8) Å). The alcoholic OH groups are deprotonated, and the alkoxo oxygens are coordinated to both Nd^{3+} in a bridging position. The Nd^{3+} ions are nine-coordinated with one water molecule per Nd(III) ion in the inner sphere. The complex $K_4[Nd_2(L\text{-}O)_2(H_2O)_2]\cdot 14H_2O$ has an inversion center, and the space group is $P\bar{1}$. Two of the K^+ counterions are six-coordinated, while the other two K^+ ions are eight-coordinated; polar polymeric water–K^+ layers are formed between the apolar ligand layers via the bridging water molecules. The dinuclear dimer complexes are also present in aqueous solution. The proton relaxivities of the Gd^{3+} complex decrease with the increase of pH, and at pH > 6, the low relaxivity values indicate the probable absence of H_2O in the inner sphere and the predominance of the eight-coordinated dimer species $[Gd_2(L\text{-}O)_2]^{4-}$. The results of ESI-TOF MS studies of the complexes of La^{3+}, Nd^{3+}, and Lu^{3+} proved the formation of dinuclear dimers in dilute (0.25 mM) solutions. pH–potentiometric titrations indicate the formation of complexes with 1:1 ($Ln(L\text{-}OH)^-$, Ln(HL-OH), and $Ln_2(L\text{-}O)_2^{4-}$) and 2:1 ($Ln_2(L\text{-}O)^+$) metal-to-ligand ratios. The stability constants of the $Ln(L\text{-}OH)^-$ species increase from La^{3+} (log K = 10.19) to Lu^{3+} (log K = 14.08). The alcoholic OH group of the $Ln(L\text{–}OH)^-$ species dissociates at unusually low pH values. The pH range of dissociation shifts to lower and lower pH's with the increasing atomic number of the lanthanides. This pH range is about 4–7 for the La^{3+} complex and 1–4 for the Lu^{3+} complex. The results of 1D and 2D ^1H and ^{13}C NMR studies of the La^{3+} complex, the number and multiplicity of signals, and the values of coupling constants are in agreement with the dinuclear dimer structure of the complex in solution.

Introduction

The complexes formed between lanthanide(III) ions and hydroxycarboxylic acids played an important role in the development of ion-exchange separation methods and the coordination chemistry of lanthanides. Citric acid was one of the first eluents used for the radiochemical and preparative chromatographic separations.[1,2] Lactic acid and particularly α-hydroxy-isobutyric acid have recently been used in analytical separations by ion exchange chromatography or capillary electrophoresis.[3−6] The successful use of these ligands for the separations has attracted considerable interest in the study of the equilibrium properties of the lanthanide-

* To whom correspondence should be addressed. E-mail: gyulat@gmail.com (G.T.); ebrucher@delfin.klte.hu (E.B.). Tel: (+1) 972-883-2666 (G.T.); (36) 52-512-900/2374 (E.B.). Fax: (+1) 972-883-2925 (G.T.); (36) 52-489-667 (E.B.).

† Department of Chemistry, Laboratory for X-ray Diffraction.

‡ Department of Inorganic and Analytical Chemistry.

§ Present address: University of Texas at Dallas, Department of Chemistry, P.O. Box 830660, Richardson, Texas 75080.

(1) Tompkins, E. R.; Mayer, S. W. *J. Am. Chem. Soc.* **1947**, *69*, 2859.
(2) Spedding, F. H.; Fulmer, E. I.; Butler, T. A.; Gladrow, E. M.; Gobush, M.; Porter, P. E.; Powell, J. E.; Wright, J. M. *J. Am. Chem. Soc.* **1947**, *69*, 2812.
(3) Choppin, G. R.; Silva, R. J. *J. Inorg. Nucl. Chem.* **1956**, *3*, 153.
(4) Nervik, W. E. *J. Phys. Chem.* **1955**, *59*, 153.
(5) Sawatari, H.; Asano, T.; Hu, X. C.; Saizuka, T.; Itoh, A.; Hirose, A.; Haraguchi, H. *Bull. Chem. Soc. Jpn.* **1995**, *68*, 898.
(6) Shi, Y. C.; Fritz, J. S. *J. Chromatogr.* **1993**, *640*, 473.

10.1021/ic0517321 CCC: $33.50
Published on Web 05/25/2006

Chart 1. Ligands Studied and Used for Comparison in This Work

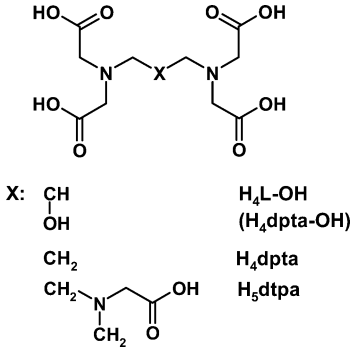

(III) (Ln^{3+}) complexes. However, despite the detailed studies, the possible role of the alcoholic hydroxyl group in the complex formation has remained a disputed problem for a long time. The stability constants of the complexes formed with, for example, glycolate, lactate, and α-hydroxy-isobutyrate are higher than those formed with acetate, propionate and isobutyrate, which indicates the role of the alcoholic hydroxyl in the complexation, but the dissociation of the coordinated OH group is disputed.[7,8] In α-hydroxy-carboxylic acids, the OH group has a terminal position, and the presence of one carboxylate group promotes the coordination of the oxygen atom of the alcoholic OH group in the complexes. In the complexes of citrate and some other hydroxy-polycarboxylates, two carboxylate groups assist not only the coordination of the alcoholic OH but also, because of the formation of two chelate rings, in the dissociation of the hydrogen ion and the coordination of the alkoxo group. The dissociation of the alcoholic OH in the La^{3+}−glycolate complex occurs at pH > 8, as was determined by NMR spectroscopy,[9] while in the Gd^{3+}−citrate complex, the dissociation takes place at pH > 5,[10] indicating the combined effect of the two coordinated carboxylates. The dissociation of the alcoholic OH in the complexes of lanthanides formed with some polyhydroxy-carboxylates has also been detected by ^{13}C NMR spectroscopy.[11]

Alcoholic hydroxyl groups are also attached to some polyamino-polycarboxylate ligands. For the complexes of *N*-2-hydroxyethyl-ethylenediamine-*N*,*N*′,*N*′-triacetate formed with La^{3+}, Lu^{3+}, and Y^{3+}, the dissociation of the alcoholic OH group was demonstrated by NMR spectroscopy.[12] However, in the lanthanide(III) complexes of the H_4edta analogue ligand, 2-hydroxy-1.3-diaminopropane-*N*,*N*,*N*′,*N*′-tetraacetic acid (H_4L-OH), which contains a linker CH(OH) group between two methyliminodiacetate groups (Chart 1), the dissociation of the alcoholic OH has not been detected either by pH potentiometry or ^1H NMR spectroscopy.[13,14] The stability constants of the Ln^{3+} complexes formed with dpta-OH are very close to those of the Ln(dpta) (H_4dpta = 1,3-diaminopropane-*N*,*N*,*N*′,*N*′-tetraacetic acid).[13,15] On the basis of these findings, Powell at al. concluded that the alcoholic OH group of L-OH does not participate in complex formation because the 2-hydroxy-1,3-diaminopropane backbone is not sufficiently flexible and the dissociation of the alcoholic OH may occur at higher pH values.[13] The complexes of L-OH formed with Fe^{3+}, Al^{3+}, and Cu^{2+} have been studied by several groups. The formation of mononuclear, dinuclear, and tetranuclear complexes with an ionized alcoholic hydroxyl group has been demonstrated.[16−18] In the di- and tetranuclear complexes, the oxygen of the ionized alcoholic OH has a μ-alkoxo bridging position. The formation of dinuclear lanthanide(III)−L-OH complexes in solution has not been detected, but the complexes formed with La^{3+} or Ce^{4+} at 2:1 metal to L-OH concentration ratio can carry out double-strand cleavage of plasmid DNA. The authors reported no information on the complexes formed in these systems. [19]

More recently it has been found by Miyashita et al. that the L-OH ligand forms dimer complexes with some lanthanides in the solid state. The X-ray diffraction studies revealed that, in the $Na_4[Yb_2(\mu\text{-L-O})_2]$ complex, the ligands are coordinated to both Yb^{3+} with an iminodiacetate group and the two Yb^{3+} ions are bridged by two alkoxo oxygens. Conductivity measurements indicated that the aqueous solution of the complex behaves like a 4:1 electrolyte.[20] The formation of a similar alkoxo-bridged dimer was found recently in the reaction of Zr(IV) and L-OH by X-ray diffraction and NMR spectroscopy.[21]

The first experiments in our study indicated the dissociation and coordination of the alcoholic OH group (formation of $Ln(L\text{-}O)^{2-}$ complexes) by pH potentiometry, and we could also detect the formation of dinuclear complexes ($Ln_2(L\text{-}O)^{+}$), which were not observed earlier.[13,14] On the basis of these interesting results, we made a detailed equilibrium study for the complexes of the whole series of lantahanides. The stoichoimetry of the complexes formed in solution was verified with ESI-TOF MS. The structures of the complexes were studied in solution by ^1H and ^{13}C NMR spectroscopy. The structure of the Nd^{3+} complex in the solid state has been studied by X-ray diffraction.

Experimental Section

Preparation of Solutions. $LnCl_3$ stock solutions were prepared by dissolving lanthanide(III) oxides (99.9% Fluka) in 6 M HCl, and the excess HCl was evaporated. The concentrations of the $LnCl_3$

(7) Choppin, G. R.; Chopoorian, J. A. *J. Inorg. Nucl. Chem.* **1961**, *22*, 97.
(8) Seyb, K. E. *J. Inorg. Nucl. Chem.* **1964**, *26*, 231.
(9) Vanwestrenen, J.; Peters, J. A.; van Bekkum, H.; Rizkalla, E. N.; Choppin, G. R. *Inorg. Chim. Acta* **1991**, *181*, 233.
(10) Jackson, G. E.; Dutoit, J. *J. Chem. Soc., Dalton Trans.* **1991**, 1463.
(11) Giroux, S.; Aury, S.; Henry, B.; Rubini, P. *Eur. J. Inorg. Chem.* **2002**, 1162.
(12) Brücher, E.; Kostromina, N. A. *Teoret. Eksper. Khim. (in Russian)* **1972**, *8*, 210.
(13) Powell, J. E.; Ling, D. R.; Tse, P. K. *Inorg. Chem.* **1986**, *25*, 585.
(14) Balgavy, P.; Novomesky, P.; Majer, J. *Inorg. Chim. Acta* **1980**, *39*, 233.
(15) Anderegg, G.; Wenk, F. *Helv. Chim. Acta* **1971**, *54*, 216.
(16) Kawata, S.; Iwaizumi, M.; Kosugi, H.; Yokoi, H. *Chem. Lett.* **1987**, 2321.
(17) Kato, M.; Yamada, Y.; Inagaki, T.; Mori, W.; Sakai, K.; Tsubomura, T.; Sato, M.; Yano, S. *Inorg. Chem.* **1995**, *34*, 2645.
(18) Schmitt, W.; Jordan, P. A.; Henderson, R. K.; Moore, G. R.; Anson, C. E.; Powell, A. K. *Coord. Chem.* Rev. **2002**, *228*, 115.
(19) Branum, M. E.; Que, L. *J. Biol. Inorg. Chem.* **1999**, *4*, 593.
(20) Miyashita, Y.; Sanada, M.; Yamada, Y.; Fujisawa, K.; Okamoto, K. *Chem. Lett.* **2002**, 840.

solutions were determined by complexometry with standardized Na_2H_2edta and xylenol orange indicator. The ligand stock solutions were prepared by dissolving H_4dpta-OH and H_4dpta (Sigma) with known amounts of KOH (pH $\approx$ 4.5). The concentration of the ligand solutions was determined by pH-potentiometric titrations in the absence and presence of a 50-fold excess of $CaCl_2$. The KCl used for keeping a constant ionic strength was recrystallyzed from double distilled water.

Equilibrium Measurements. The pH−potentiometric titrations were carried out with a Radiometer PHM-85 pH meter, using pHG211 glass and K401calomel electrodes in vessels thermostated at 25 °C. The titrations were made with an ABU80 autoburet. The titrated samples (20 mL) were stirred with a magnetic stirrer, and argon gas was bubbled throughout the measurements. For the calibration of the electrode system, KH−phthalate (pH = 4.005) and Borax (pH = 9.180) buffers were used. To obtain H^+ concentrations from the measured pH values, the method proposed by Irving et al. was used.[22] A 0.01 M HCl solution (1.0 M for KCl) was titrated with standardized KOH solution. The differences between the measured and calculated pH values were used to calculate the H^+ concentrations from the pH values, measured in the titration experiments. The ionic product of water (log K_w) was found to be 13.89. The concentration of the ligand solutions titrated in the presence of $LnCl_3$ varied between 0.002 and 0.01 M. The metal to ligand concentration ratio was 4, 2, 1, 0.67, 0.5, and 0.25 for La, Eu, Ho, Er, Tm, Lu, and Y; 4, 2, 1, and 0.25 for Nd, Gd, Tb, Dy, and Yb; and 2, 1, and 0.5 for the Ce, Pr, and Sm. The number of the fitted milliliters of titrant−pH ([H^+]) data points used for the equilibrium calculations was between 150 and 520. For the titrations, 0.2 M KOH, which was kept under argon atmosphere, was used. The ionic strength of the titrated solutions was constant, 1.0 M for KCl. The protonation constants of the ligand ant stability constants of the complexes were calculated with the use of the computer program PSEQUAD.[23]

Spectrophotometric measurements were made with a Cary 1E UV−vis spectrophotometer using 5 cm cells in a thermostated cell holder.

Preparation of the $K_4[Nd_2(L\text{-}O)_2(H_2O)_2]\cdot 14H_2O$ Complex. Equivalent amounts (0.3 mmol) of the K_2H_2L-OH ligand and $NdCl_3$ stock solutions were mixed together, and the pH of the mixture was increased to about 7.5 with the addition of KOH solution. On the basis of the equilibrium studies at this pH, only the $[Nd_2(L\text{-}O)_2]^{4-}$ species is present in the solution. Absolute ethanol was added to the solution of the complex when the complex quickly solidified in the form of a pinkish powder. The precipitate was filtered and washed twice with anhydrous ethanol (10 mL) and diethyl ether (10 mL) and dried in air to a constant weight. A weighted amount (0.047 g, 0.1 mmol) of the dried complex was redissolved in 0.5 mL of doubled distilled water and placed into a narrow tube. Anhydrous ethanol was carefully layered on the aqueous phase, and the tube was placed into refrigerator and maintained at around 4 °C. Pink block crystals suitable for X-ray crystallography grew in three weeks.

X-ray Crystallography. A pink block crystal of $K_4[Nd_2(L\text{-}O)_2(H_2O)_2]\cdot 14H_2O$ was mounted into a capillary to prevent drying and deterioration of the crystal. Data were collected at 293(1)K on an Euraf Nonius MACH3 diffractometer using monochromated Mo Kα radiation (λ = 0.71073 Å) and $\omega-2\theta$ motion. Absorption corrections were made using ψ scans. The structure was solved using direct methods with SIR-92 software, and refined on F^2 by full-matrix least-squares methods using SHELX-97.[24,25] All non-hydrogen atoms were refined anisotropically. Hydrogen atoms of the C−H were included using a riding model. Some of the water hydrogen atoms were found on the difference electron density map, while others were placed into calculated positions for strong hydrogen bonds. For the final refinement, O−H bond distances were restrained for 0.85 Å. Publication material was prepared with the WINGX-97 suite.[26] The residual electron density of 1.162−1.453 e/Å is close to the neodimium atom (<1 Å).

Measurement of Relaxation Times. The longitudinal relaxation times of the water protons (T_1) in the presence of $Gd(L\text{-}OH)^-$ and $Gd(dpta)^-$ were measured with an MS-4 NMR spectrometer (Institute Jozef Stefan, Ljubljana) at 9 MHz. The temperature of the cell holder was controlled with a thermostated air stream. The T_1 values were measured by the inversion recovery method (180°−τ−90°) with five to nine measurements at six to eight different τ values at 25 °C. The concentration of the Gd^{3+} complex solution was 1.0 mM.

Electrospray Ionization Time-of-Flight Mass Spectrometry (ESI-TOF MS). ESI-TOF MS measurements were performed on a BioTOF II instrument (Bruker Daltonics, Billerica, MA). The solutions were introduced directly into the ESI source by a syringe pump (Cole-Parmer Ins. Co.) at a flow rate of 2 μL/min. The temperature of drying gas (N_2) was maintained at 100 °C. The voltages applied on the capillary entrance, capillary exit, and the first and the second skimmers were −4500, 120, 40, and 30 V, respectively. The spectra were accumulated and recorded by a digitizer at a sampling rate of 2 GHz.

NMR Spectroscopy. The solutions of complexes were prepared by mixing equivalent amounts of the K_2H_2L-OH and $LnCl_3$ solutions. After evaporation of the H_2O, the solid material was dissolved in D_2O. The pD of the solutions was monitored by the addition of KOD or DCl (Cambridge Isotope Laboratories) solutions, and the readings were corrected for the deuterium isotope effect using the relationship pH = 0.4 + pD.[27] Both one- and two-dimensional NMR spectra were recorded mainly on a Bruker Avance DRX-360 spectrometer operating at 360.0 and 90.5 MHz for ^{1}H and ^{13}C, respectively. Chemical shifts were referenced to the signal of DSS (DSS = 2,2-dimethyl-2-silapentane-5-sulfonate) in D_2O as an internal standard. For variable-temperature measurements, a Bruker DRX-500 spectrometer was used. It was equipped with Eurotherm variable-temperature unit (±0.1 K), which was calibrated using the methanol method.[28] Two-dimensional ^{1}H−^{1}H correlation spectroscopy (COSY-45, DQF−COSY, NOESY, and EXSY) and ^{1}H−^{13}C heteronuclear shift correlation spectra (HETCOR and COLOC) were recorded using standard pulse sequences in direct mode with a 5 mm QNP probehead. The repetition times between two transients were as long as possible but not less than 5 and 30 s for ^{1}H and ^{13}C nuclei, respectively, to get the proton and carbon atoms relaxed. ^{13}C NMR spectra were recorded in *J*-modulated or inverse-gated decoupling mode. The NOESY and EXSY spectra were recorded in TPPI mode (TPPI = time-

(21) Zhong, W. Q.; Parkinson, J. A.; Parsons, S.; Oswald, L. D. H.; Coxall, R. A.; Sadler, P. J. *Inorg. Chem.* **2004**, *43*, 3561.
(22) Irving, H. M.; Miles, M. G.; Pettit, L. D. *Anal. Chim. Acta* **1967**, *38*, 475.
(23) Zékány, L.; Nagypál, I. *Computational Methods for Determination of Formation Constants*; Legett, D. J., Ed.; Plenum Press: New York, 1985.
(24) Altomare, A.; Cascarano, G.; Giacovazzo, C.; Guagliardi, A. *J. Appl. Crystallogr.* **1993**, *26*, 343.
(25) Sheldrik, G. M.; *SHELX-97, A Program for Crystal Structure Refinement*; University of Göttingen: Göttingen, Germany, 1997.
(26) Farrugia, L. J.; *WINGX-97 system*; University of Glasgow: Glasgow, U.K. 1996.
(27) Mikkelsen, K.; Nielsen, S. O. *J. Phys. Chem.* **1960**, *64*, 632.
(28) Van Geet, A. L. *Anal. Chem.* **1970**, *42*, 679.

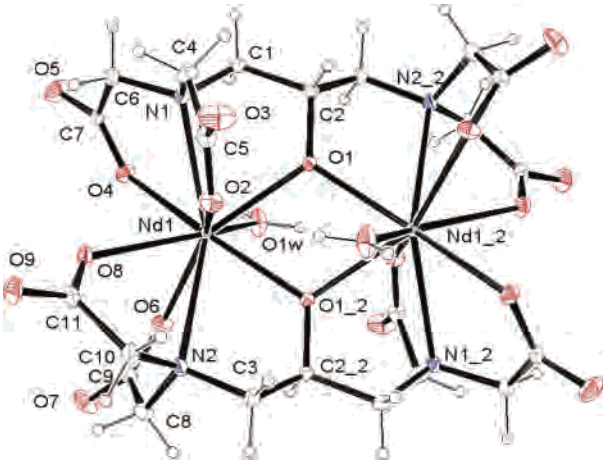

Figure 1. ORTEP view of the structure of $K_4[Nd_2(L\text{-}O)_2(H_2O)_2]$ at the 35% probability level with a partial numbering scheme. Solvent water molecules and potassium ions are omitted for clarity.

Table 1. Details of X-ray Data Collection and Structure Refinement for $K_4[Nd_2(L\text{-}O)_2(H_2O)_2]\cdot 14H_2O$

chemical formula	$C_{11}H_{29}K_2N_2O_{17}Nd$
mol wt	683.8
cryst habit	pink block
cryst size (mm^3)	0.40 × 0.35 × 0.32
cryst syst	triclinic
space group	$P\bar{1}$
a (Å)	9.5072(10)
b (Å)	10.2779(10)
c (Å)	13.497(2)
α (deg)	78.69(1)
β (deg)	71.95(1)
γ (deg)	82.48(1)
V ($Å^3$)	1226.1(3)
Z	2
T (K)	293
ρ_{calcd} (g cm^{-3})	1.852
μ (mm^{-1})	2.534
F (000)	686
$2\theta_{max}$ (deg)	50.74
no. reflns collected	4854
no. unique reflns with $I > 2\sigma(I)$	4495
params	346
R^a	0.0327
R_w (all data)^b	0.1365
GOF on F^2	1.503

[a] $R = \sum|F_o - F_c|/\sum F_o$. [b] $R_w = \{\sum[w(F_o^2 - F_c^2).^2]/\sum[w(F_o^2).^2]\}^{1/2}$, where $w = 1/[\sigma^2(F_o^2 + (aP)^2 + bP)]$, $P = (F_o^2 + 2F_c^2)/3$, and a and b are constants given in the Supporting Information.

proportional phase incrementation) and at least 3 times with various mixing times to obtain acceptable noesy spectra.

Data processing was performed mainly with the Bruker WinNMR program package. For the preparation of the electronic Supporting Information, the program MestReC (beta version) was used.

Results and Discussion

X-ray Crystal Structure. The structure of $K_4[Nd_2(L\text{-}O)_2(H_2O)_2]\cdot 14H_2O$ has been established by single-crystal X-ray diffraction studies (Figure 1 and Tables 1 and 2). The solid-state structure inevitably shows deprotonation of the alcoholic OH group and formation of a dimeric complex in which the two $(L\text{-}O)^{5-}$ ligands are coordinated to both Nd^{3+} with an imda group and the bridging alkoxo oxygen. The similar $[Yb_2(L\text{-}O)_2]^{4-}$ complex is also a dimer having crystallographic mirror plane between the two metal atoms.[20]

Table 2. Selected Bond Lengths (Å) and Angles (deg) for $K_4[Nd_2(L\text{-}O)_2(H_2O)_2]\cdot 14H_2O$[a]

Nd1−Nd1^{i}	3.9283(8)	Nd1−O1w	2.559(6)
Nd1−O1	2.379(5)	Nd1−O1^{i}	2.325(4)
Nd1−O2	2.476(5)	Nd1−N1	2.691(5)
Nd1−O4	2.497(5)	Nd1−N2	2.802(6)
Nd1−O6	2.468(5)	O1−C2	1.403(8)
Nd1−O8	2.475(5)	Nd1−K1^{ii}	4.560(2)
K2−K2^{iii}	3.656(4)		
O1−Nd1−O1^{i}	66.8(2)	O1−Nd1−O4	109.45(2)
Nd1−O1−Nd1^{i}	113.2(2)	O1−Nd1−O6	140.1(2)
O1−Nd1−N1	64.9(2)	O1−Nd1−O8	142.4(2)
O1−Nd1−N2	125.3(2)	N1−Nd1−N2	136.6(2)
O1−Nd1−O1w	74.2(2)	O1w−Nd1−Nd1^{i}	76.5(1)

[a] For numbering scheme see Figure 1. Symmetry transformation used to generate equivalent atoms: i $1-x, 1-y, -z$; ii $1-x, -y, -z$; iii $-x, -y, 1-z$.

However, in our case, the solid-state structure of the Nd^{3+} complex has lower symmetry with inversion center and the space group is $P\bar{1}$, triclinic. The lack of higher symmetry can be explained as the two imino-diacetate groups of the ligand are not equivalent having different electrostatic interactions and hydrogen-bond networks (see later). As a result of its ionic radius, the coordination number of Nd^{3+} is 9 (i.e., apart from two imino-diacetate fragments and two bridging alkoxy groups a water molecule (O1w) is coordinated). Because of steric reasons, the Nd−N distances differ for the two amino-polycarboxylate ligands giving 2.691(5) and 2.802(6) Å. Altogether the coordination of neodimium is highly disordered, the Nd−Nd distance being 3.9283(8) Å. It is worth to mention that in a similar dimeric vanadyl complex of the same ligand the V−V distance is 3.343(2) Å,[29] while the same data for an iron complex is 3.305(2) Å.[30] Miyashita et al. crystallized and collected X-ray data for the holmium and ytterbium complexes too, giving 3.646(2) and 3.716(5) Å, respectively, as the metal−metal distances for the dimers.[20] These numbers indicate that the $(L\text{-}O)^{5-}$ ligand is quite relaxed in our Nd^{3+} complex. Strong electrostatic interactions, as well as a hydrogen-bond network, stabilize the structure. Data for the hydrogen-bond network are given as Supplementary Information (Table S1). One of the potassium counterions has distorted octahedral coordination to the non-Nd-coordinated oxygen atoms of the acetate arms and bridging water molecules to the symmetry-related potassium (K−K = 3.656(4) Å), while there are 8 potential donor atoms around the second potassium ion with bridging O1w, O4, and O6 to the nearest neodimium atom (K−Nd = 4.560(2) Å). Altogether the structure is a complicated polymeric one with polar water−potassium regions between apolar ligand layers.

Equilibrium Studies. The protonation constants of the ligand L-OH ($K_i^H = [H_iL]/[H_{i-1}L][H^+]$) have been determined by pH−potentiometric titration of 0.005 and 0.01 M solutions. The log K_i^H values were calculated with the use of 284 data points obtained in the pH range of 1.6−11.0. The log K_i^H values (and the standard deviations) are pre-

(29) Robles, J. C.; Matsuzaka, Y.; Inomata, S.; Shimoi, M.; Mori, W.; Ogino, H. *Inorg. Chem.* **1993**, *32*, 13.
(30) Schmitt, W.; Anson, C. E.; Pilawa, B.; Powell, A. K. *Z. Anorg. Allg. Chem.* **2002**, *628*, 2443.

Table 3. Protonation Constants of the Ligands L-OH[a] and dpta[b]

log K_i^H	L-OH[a]	L-OH[b]	dpta[c]
log K_1^H	9.19 (0.01)	9.49	10.46
log K_2^H	6.87 (0.01)	7.04	8.02
log K_3^H	2.46 (0.01)	2.62	2.47
log K_4^H	1.76 (0.01)	1.47	1.88
log K_5^H	1.5 (0.01)		

[a] t =25 °C, I = 1.0 M KCl. [b] 25 °C, 0.1 M KNO_3, ref 13. [c] I = 0.1 M KNO_3, ref 15.

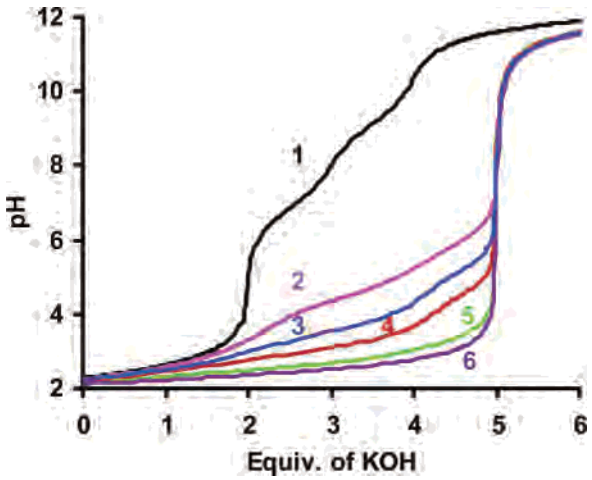

Figure 2. Titration curves of the H_4L-OH ligand (2.0×10^{-3} M) in the absence (1) and presence of equivalent amounts of La^{3+} (2), Nd^{3+} (3), Gd^{3+} (4), Er^{3+} (5), and Lu^{3+} (6).

sented in Table 3. For comparison, the protonation constants reported by Powell at al.[13] and the log K_i^H values of the analogous ligand dpta[15] are also shown in Table 3. The log K_i^H values obtained at lower ionic strength (0.1 M KNO_3) are about 0.2−0.3 log K unit higher than those determined by us in 1.0 M KCl. These discrepancies are caused by the difference in the ionic strengths and the more prominent complexation with K^+ at 1.0 M concentration. The first two protonation constants of L-OH are significantly lower than those of the structurally similar dpta (Chart 1). The lower basicity of the two nitrogen atoms of L-OH is probably the result of the electron-withdrawing effect of the oxygen atom of the alcoholic OH.

The dissociation of the alcoholic OH group of the free ligand could not be detected by ^{1}H NMR spectroscopy. The effect of increasing OH^- ion concentration on the ^{1}H NMR spectra of the ligand have been studied in the range of 0.01−2.5 M (the sum of the KOH and KCl concentration was 3.0 M). The signals, involving that of the methyne proton (CH−OH) and methylene protons of the acetate arms (N−CH_2−COO^-), were both shifted very slightly upfield with increasing OH^- concentration, which indicated that the dissociation of the alcoholic hydroxyl group of the free ligand does not take place even in 2.5 M KOH.

The pH−potentiometric titration curves of the L-OH ligand obtained in the presence and absence of the Ln^{3+} ions are shown in Figure 2. The titration data indicate that 5 equiv of KOH were needed for the neutralization of all the dissociable protons of L-OH at a 1:1 metal-to-ligand ratio. While the addition of the fifth equivalent of base results in a weaker jump in the titration curves of the lighter lanthanides, the pH values obtained in the presence of heavier lanthanides (Er^{3+} and Lu^{3+} in Figure 2) show a smooth increase, and the base consumption is finished at a pH of around 4−5. At such low pH values, the hydrolysis of lanthanides cannot occur, thus the fifth equivalent of base is used to neutralize the protons released by the ionization of the alcoholic OH group. The neutralization of the alcoholic OH occurs in lower and lower pH ranges as the atomic number of the lanthanides increases. For La(L-OH), it occurs in the pH range of about 4−7, while for the Lu(L-OH), the neutralization is practically finished at around pH 4. According to these observations the interaction between the Ln^{3+} ion and the alkoxo oxygen O^- is electrostatic in nature which becomes stronger with the decrease of the size of the Ln^{3+} ions. The dissociation of the alcoholic OH in the L-OH complexes was not taken into account by Powell et al., even at pH values of about 4−5, and they assumed the formation of the Ln(L-OH)$^-$ species only. [13]

To obtain information on the composition of the complexes formed in the Ln^{3+}−L-OH systems, spectrophotometric studies were performed. The narrow absorption band of Nd^{3+} (aq) observed at 427.1 nm ($^2P_{1/2}$−$^4I_{9/2}$ transition) is very sensitive for the changes in its surroundings.[31] At a 1:1 concentration ratio of Nd^{3+} and L-OH at pH values above 2, a new band appears at 428.4 nm. The intensity of this band increases with increasing pH, and at about pH 3, another band starts to appear at 430.2 nm. The position of the first band is close to that of the Nd(mimda)$^+$ band (428.3 nm), which indicates that at about pH 2−3 a protonated complex is formed when an iminodiacetate group and probably the oxygen of the alcoholic OH is coordinated to the Nd^{3+} while the other iminodiacetate group is free. The band at 430.2 nm is presumably characteristic of the formation of the species Nd(L-OH)$^-$, in which all the donor atoms of the ligand are coordinated, since, in the case of Nd(edta)$^-$, the band appears at 429.5 nm and the coordination of the alcoholic OH may result in a red shift. These results indicate the formation of the Nd(L-OH)$^-$ complex in the pH range of about 3−5. Above pH 4.5, a new band appears at about 430.8 nm. The shape and position of this band does not change between pH 6 and 13, indicating that the Nd(L−O)$^{2-}$ complex, formed by the ionization of the alcoholic OH group, exists in this broad pH range.

In the presence of excess Nd^{3+} (0.01 M Nd^{3+} and 0.005 M L-OH), the intensity of the band characteristic for the Nd^{3+} (aq) decreases with the increase of pH and practically disappears at about pH > 6.3, indicating the formation of dinuclear complexes with a broad absorption band at about 429 nm. From the solution at a pH of ∼6.3, nearly the total amount of the complex was precipitated in several hours. The composition of the precipitate was studied pH potentiometrically and found to be Nd_2(L-O)(OH). The precipitate could be dissolved by adding KOH at about a pH of 9−10, and the solution obtained was stable even at pH around 12.

(31) (a) Yatsimirskii, K. B.; Davidenko, N. K.; Kostromina, N. A.; Ternovaya, T. V. *Teoret. Eksper. Khim. (in Russian)* **1965**, *1*, 100. (b) Kostromina, N. A.; Slovatsevskaya, E. M. *Zh. Inorg. Chem. (in Russian)* **1968,** *13*, 1105.

The solution had a broad absorption band with a maximum at 429.8 nm.

In the presence of a large (20-fold) ligand excess at different pH values, the Nd^{3+} spectra were identical to those obtained at a 1:1 metal-to-ligand ratio, indicating that complexes with 1:2 metal-to-ligand ratios were not formed. The formation of ternary complexes between $Nd(L-O)^-$ and excess imda, glycinate, or salicylate ligands could not be detected by spectrophotometry. The absence of ternary complex formation indicates that the number of free coordination sites on the Nd^{3+} is lower than two: it is either one or zero. This is in good agreement with the number of coordinated water molecules (q), which was found to be 0.50 for the $Eu_2(L-O)_2^{4-}$ complex, determined by fluorescence lifetime measurements using the method proposed by Beeby et al.,[32] and also with the unusually low relaxivity value obtained for the $Gd_2(L-O)_2^{4-}$ complex (vide infra).

On the basis of the results obtained by pH potentiometry and spectrophotometry, we assumed the formation of protonated Ln(HL-OH) and nonprotonated $Ln(L-OH)^-$ complexes. The dissociation of the alcoholic OH group may lead to the formation of the $Ln(L-O)^{2-}$ species. In the presence of excess Ln^{3+}, dinuclear $Ln_2(L-O)^+$ complexes can be formed. Since the solubility of the dinuclear complexes in the pH range of about 6.5−9 is low and the formation of some hydroxo species is slow, we only calculated the stability constant of the $Ln_2(L-O)^+$ complex, which is formed at pH < 6. The stability constants characterizing the assumed equilibria are as follows:

$$K_{Ln(L-OH)^-} = \frac{[Ln(L-OH)^-]}{[Ln^{3+}][L-OH^{4-}]} \quad (1)$$

$$K_{Ln(HL-OH)} = \frac{[Ln(HL-OH)]}{[Ln(L-OH)^-][H^+]} \quad (2)$$

Because the dissociation constant characterizing the ionization of the alcoholic OH group of the ligand cannot be determined, the stability constant of the species $Ln(L-O)^{2-}$ cannot be calculated. The formation of this species is characterized with the reciprocal of the dissociation constant of the species $Ln(L-OH)^-$

$$K_{Ln(L-O)^{2-}} = \frac{[Ln(L-OH)^-]}{[Ln(L-O)^{2-}][H^+]} \quad (3)$$

The stability constant of the dinuclear complex is defined as

$$K_{Ln_2(L-O)^+} = \frac{[Ln_2(L-O)^+]}{[Ln(L-O)^{2-}][Ln^{3+}]} \quad (4)$$

The formation of the protonated complexes is important only for the lighter lanthanides (to Tb^{3+}). However, for the description of the equilibria for the La^{3+}, Ce^{3+}, Pr^{3+}, and Nd^{3+} complexes, the assumption for the formation of diprotonated species $Ln(H_2L-OH)^+$ leads to better fitting parameters and lower standard deviation values. For the complexation of Nd^{3+}, the spectrophotometric data and the calculated species distributions agreed only if the formation of the diprotonated species was taken into consideration by the calculations.

Table 4. Stability Constants (log K) of Complexes Formed in the Ln^{3+}−L-OH System[a]

Ln	$Ln(L-OH)^-$	Ln(HL-OH)	$Ln(L-O)^-$	$Ln_2(L-O)_2^{4-}$	$Ln_2(L-O)^+$
La	10.19(0.01)	4.39(0.02)	5.71(0.02)	9.01(0.03)	4.22(0.03)
Ce	10.93(0.03)	3.77(0.05)	5.18(0.03)	8.03(0.06)	4.53(0.10)
Pr	11.87(0.03)	3.28(0.05)	4.99(0.02)	7.61(0.05)	4.68(0.07)
Nd	12.08(0.02)	3.12(0.04)	4.73(0.02)	7.13(0.05)	4.02(0.05)
Sm	12.56(0.04)	2.94(0.06)	4.26(0.03)	6.12(0.07)	4.28(0.11)
Eu	12.86(0.02)	2.75(0.04)	4.17(0.02)	5.99(0.05)	4.20(0.05)
Gd	12.82(0.02)	2.56(0.06)	4.09(0.02)	5.89(0.05)	3.82(0.06)
Tb	13.24(0.02)		3.78(0.02)	5.21(0.05)	3.61(0.06)
Dy	13.56(0.02)		3.54(0.02)	4.70(0.05)	3.49(0.06)
Ho	13.57(0.02)		3.24(0.02)	4.01(0.04)	2.80(0.05)
Er	13.71(0.02)		2.87(0.02)	3.31(0.04)	2.30(0.06)
Tm	13.84(0.04)		2.38(0.03)	2.52(0.04)	2.48(0.05)
Yb	14.38(0.03)		2.07(0.01)	2.08(0.02)	2.48(0.02)
Lu	14.08(0.01)		2.09(0.01)	2.12(0.01)	1.69(0.03)
Y	12.79(0.02)		3.11(0.01)	3.91(0.03)	1.66(0.07)

[a] t = 25 °C, I = 1.0 M KCl.

The experimental data obtained by ESI-TOF MS and NMR spectroscopy indicated that parallel with the dissociation of the alcoholic OH group, dimer complexes of $Ln_2(L-O)_2^{4-}$ were formed, and the dimerization was practically complete even in dilute (0.25 mM) solutions. The dissociation of the alcoholic OH group and the formation of dimer complexes can be characterized with the equilibrium as follows:

$$2Ln(L-OH)^- \rightleftharpoons Ln_2(L-O)_2^{4-} + 2H^+ \quad (5)$$

This equilibrium is characterized by the equilibrium constant $K_{Ln_2(L-O)_2^{4-}}$

$$K_{Ln_2(L-O)_2^{4-}} = \frac{[Ln_2(L-O)_2^{4-}][H^+]^2}{[Ln(L-OH)^-]^2} \quad (6)$$

The equilibrium constant $K_{Ln_2(L-O)_2^{4-}}$ is a composite constant that expresses the propensity of the $Ln(L-OH)^-$ complexes for both the dissociation of the alcoholic OH and the structural rearrangement to form a dimer species. The dimerization may also promote the dissociation of the OH group. Thus the equilibrium constant $K_{Ln_2(L-O)_2^{4-}}$ (defined by eq 6) has a physical meaning, while $K_{Ln(L-O)^{2-}}$ is a formal constant. However, the $K_{Ln(L-O)^{2-}}$ values can be used for practical aims such as to express, for example, more directly the extent of dissociation of the alcoholic OH at different pH values, and so with the other equilibrium constants, we also present the log $K_{Ln(L-O)^{2-}}$ values in Table 4. It is quite surprising that the log $K_{Ln(L-O)^{2-}}$ values are unusually low and the $Ln(L-OH)^-$ complexes behave like medium-weak acids. The significant decrease in the log $K_{Ln(L-O)^{2-}}$ values from La to Lu indicates that the interaction between the alkoxo oxygen and the Ln^{3+} ions increases with the decrease of the ionic size of lanthanides. The low log $K_{Ln(L-O)^{2-}}$ values are probably the result of the cooperative effect of all the functional groups of the ligand. The two coordinated

(32) Beeby, A.; Clarkson, I. M.; Dickins, R. S.; Faulkner, S.; Parker, D.; Royle, L.; de Sousa, A. S.; Williams, J. A. G.; Woods, M. *J. Chem. Soc., Perkin Trans. 2* **1999**, 493.

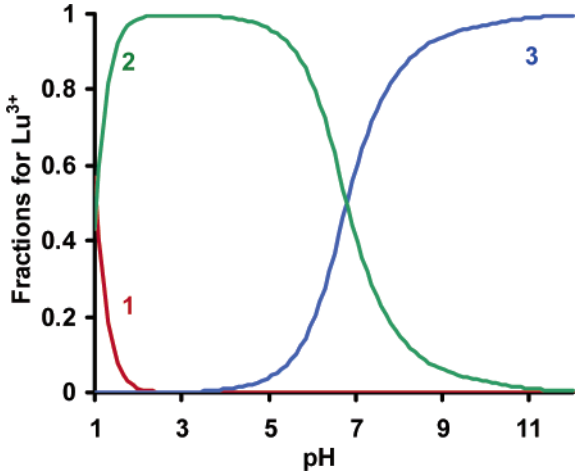

Figure 3. Species distribution in the Lu^{3+}−L-OH−edta system (the concentrations of all reacting species were 5 mM). Numbers refers to the species Lu^{3+} (1), $Lu(edta)^-$ (2), and $Lu_2(L\text{-}O)_2^{4-}$ (3) (the concentrations of other species in the equilibrium model were too low to appear).

iminodiacetate groups in $Ln(L\text{-}OH)^-$ pull the alcoholic OH close to the Ln^{3+} ion, and the formation of two chelate rings with the $N-CH_2-CH(OH)-CH_2-N$ amine chain leads to a strong electrostatic interaction between the OH oxygen and the Ln^{3+} ion, resulting in the weakening of the O−H bond and the dissociation of the H^+.

The increase in the relative stability of the $Ln_2(L\text{-}O)_2^{4-}$ complexes resulting from the coordination of the ionized alcoholic OH group can be demonstrated by calculating the species distributions in the presence of the Ln^{3+} ion, L-OH, and edta at a 1:1:1 concentration ratio. As can be seen in Figure 3, for the complexation of Lu^{3+} the species, $Lu(edta)^-$ predominates between pH 2 and 6 since its stability constant, $\log K_{Lu(edta)^-} = 19.8$ is significantly higher than that of $Lu(L\text{-}OH)^-$ (Table 4).[33] However at pH > 5, the $(L\text{-}O)^{5-}$ ligand starts to replace the edta, and at pH > 8, the $Lu_2(L\text{-}O)_2^{4-}$ species dominates. In the case of lanthanides of lower atomic number, the displacement of edta occurs at a higher pH range.

The stability constants of the $Ln(L\text{-}OH)^-$ complexes determined by Powell et al.[13] are somewhat higher for the whole series of lanthanides than the $\log K_{Ln(L-OH)^-}$ values obtained by us (Figure 4). The differences are partly from the higher protonation constants (Table 3), but the increase in the differences upon going from La^{3+} to Lu^{3+} is the consequence of the dissociation of the alcoholic OH group which was not taken into account by Powell et al.[13]

Relaxometric Studies. The relaxation rate of water protons, $1/T_1$ (T_1 is the longitudinal relaxation time), significantly increases in the presence of paramagnetic Gd^{3+} complexes. The increase in the $1/T_1$ values produced by the increase in the concentration of the Gd^{3+} complex by 1.0 mM is called the relaxivity (r_1, $mM^{-1}\ s^{-1}$) of the solution. The relaxivity is composed of the inner-sphere (r_1^{is}) and outer-sphere (r_1^{os}) terms. The inner-sphere relaxivity occurs as the water molecules coordinated in the inner sphere of Gd^{3+} exchange rapidly with the bulk water. The outer-sphere relaxivity is the result of the diffusion of the water molecules in the proximity of the Gd^{3+}-containing species. The relaxation effect of the Gd^{3+} complexes strongly depends on the number of water molecules coordinated in the inner sphere of Gd^{3+} (r_1^{is}). The numbers of inner-sphere water molecules in the complexes $Gd(dpta)^-$, $Gd(dtpa)^{2-}$ and $Gd(ttha)^{3-}$ (H_6ttha = triethylene-tetramine hexaacetic acid) are two, one, and zero, respectively, and the relaxivity values (9 MHz, 25 °C) are 9.1, 5.8, and 2.9 $mM^{-1}\ s^{-1}$, respectively.[34,35]

The relaxivity values obtained for the Gd^{3+}−L-OH and Gd^{3+}−dpta systems at different pH values at 9 MHz (25 °C) are shown in Figure 5. The formation of $Gd(dpta)^-$ occurs in the pH range of about 3−5, where the relaxivity values significantly decrease. In the Gd^{3+}−L-OH system, the drop in the relaxivity values starts at about pH 2, indicating the formation of the Gd(HL-OH) and $Gd(L\text{-}OH)^-$ species. However, at somewhat higher pH values, the dissociation of the alcoholic OH group starts and finishes at about pH 6 when the ligand $L\text{-}O^{5-}$ coordinates to the Gd^{3+} by its seven donor atoms. By the formation of a Gd^{3+}complex with a heptadentate ligand, the relaxivity value should be higher than that of the $Gd(dtpa)^{2-}$ in which the ligand is octadentate and there is only one water molecule in the inner sphere. Surprisingly, at pH > 6 when the predominance of the $Gd(L\text{-}O)^{2-}$ species is expected, the relaxivity value is around 3.4 $mM^{-1}s^{-1}$, which is significantly lower than that of $Gd(dtpa)^{2-}$. This unexpectedly low relaxivity value cannot be interpreted by assuming the slow exchange of the coordinated water(s), as was observed for the Gd^{3+}complexes formed with some dtpa- and dota-amide derivatives (H_4dota = 1,4,7,10-tetraazacyclododecane-1,4,7,10-tetraacetic acid), because the increase of temperature results in a smooth decrease in the relaxivity values of $Gd(L\text{-}O)^{2-}$, similar to that of $Gd(dtpa)^{2-}$ and $Gd(dota)^-$ (Figure S1).[36,37] The interpretation of the low relaxivity is possible by assuming the formation of dimer complexes, $Gd_2(L\text{-}O)_2^{4-}$, in solution, in which there are no water molecule in the inner sphere of Gd^{3+}, similar to $Yb_2(L\text{-}O)_2^{4-}$ found in solid state by Miyashita et al.[20] The relaxivity values increase linearly with the increase of the concentration of the Gd^{3+} complex in the range of 0.5−10 mM at pH 7.8, which indicates that the composition of the $Gd_2(L\text{-}O)_2^{4-}$ complex does not change in this concentration range (Figure S2).

ESI-TOF MS Studies. Electrospray mass spectrometry is increasingly used to study the stoichiometry of metal complexes formed in dilute solutions by transferring and identifying them in the gas phase. The passage into the gas phase is a gentle process where the metal−ligand composition of the solution species does not change. Anionic

(33) Martell, A. E.; Smith, R. M. *Critical Stability Constants*, Vol. 1; Plenum: New York, 1974.

(34) Southwood-Jones, R. V.; Earl, W. L.; Newman, K. E.; Merbach, A. E. *J. Chem. Phys.* **1980**, *73*, 5909.

(35) Caravan, P.; Ellison, J. J.; McMurry, T. J.; Lauffer, R. B. *Chem. Rev.* **1999**, *99*, 2293.

(36) Aime, S.; Botta, M.; Fasano, M.; Paoletti, S.; Analli, P. L.; Mggeri, F.; Virtuani, M. *Inorg. Chem.* **1994**, *33*, 4707.

(37) Dunand, F. A.; Aime, S.; Merbach, A. E. *J. Am. Chem. Soc.* **2000**, *122*, 1506.

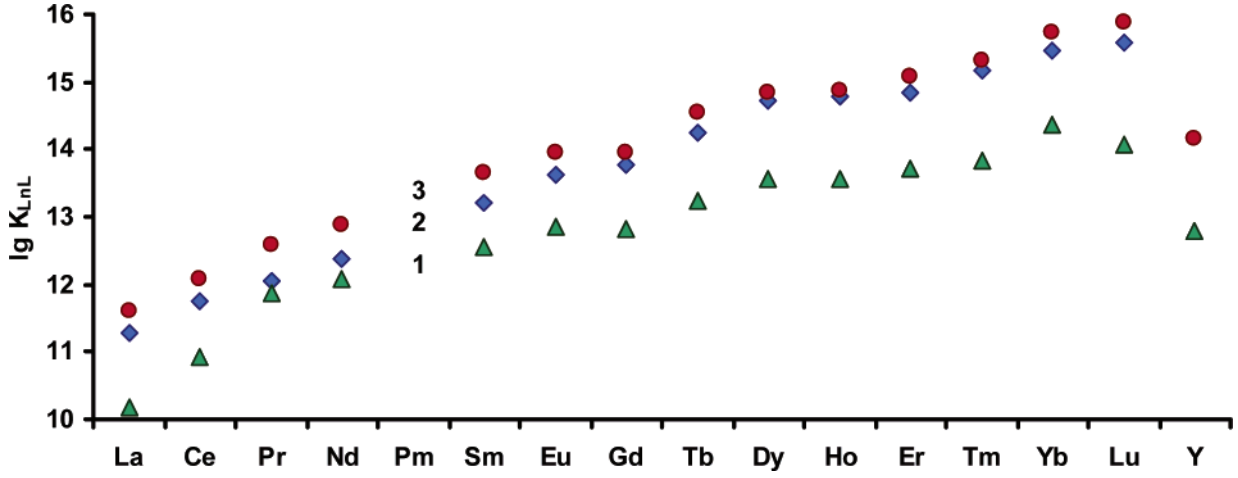

Figure 4. Comparison of the stability constants of complexes formed with L-OH [(1) this work, (3) ref 13] and dpta [(2) ref 15].

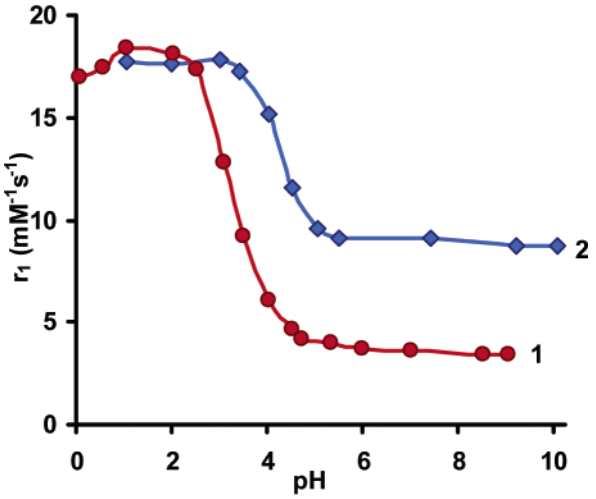

Figure 5. Relaxivities of water protons in the Gd^{3+}−L-OH (1) and Gd^{3+}−dpta (2) systems at 9 MHz and 25 °C (the Gd^{3+} and ligand concentrations were 1 mM).

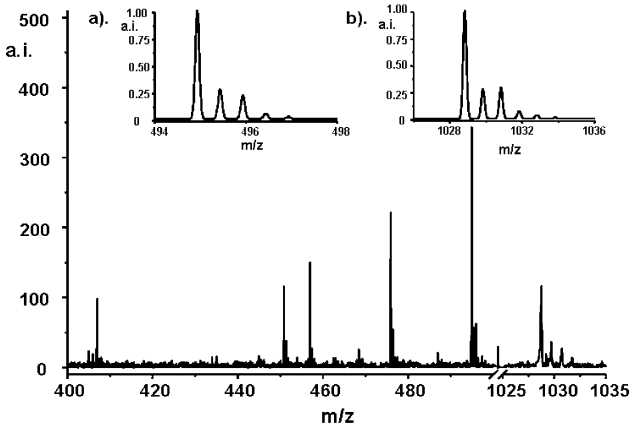

Figure 6. ESI-TOF MS spectrum of the solution containing equimolar amounts of La^{3+} and L-OH (0.25 mM and pH = 8.47). The insert spectra shows (a) the isotope distribution calculated for the dimer species $K_3La_2(L\text{-}O_2)^-$ and (b) the isotope distribution calculated for the dimer species $K_2La_2(L\text{-}O)_2^{2-}$. The isotope distributions for the other parts of the spectra are also satisfactory.

complexes may interact in the gas phase with positive ions, like alkali metals or protons. The interaction with protons is more probable if the solution is acidic or neutral. The complexes formed with polycarboxylate ligands can undergo decarboxylation, when one or more CO_2 molecules are lost.[38]

The dimerization of the Ln(III)−aminopolycarboxylate complexes in solution, which had to be assumed for the interpretation of the results of relaxivity measurements, is quite unusual. To obtain information with an independent method, detailed ESI-TOF MS studies were made on the La^{3+}, Nd^{3+}, and Lu^{3+} complexes to find out if the dimer structure is retained in solution. In the samples studied, the concentration of the Ln^{3+} ion and the L-OH ligand were 0.25 mM, and the pH was around 8, where the dissociation of the alcoholic OH group was practically complete for all complexes studied and the presence of single dimer species was expected in solution on the basis of equilibrium studies. Because of the negative charge of the complexes, the ESI MS spectra were recorded in negative ion mode.

The spectrum obtained for the La complex (Figure 6) shows six peak groups in the region of 400−1100 *m*/*z* with a characteristic isotopic distribution for the species containing the $La_2(L\text{-}O)_2^{4-}$ unit. The peaks were assigned as follows: peaks at around 1028.7−1031.7 *m*/*z* with frequency of 1 *m*/*z* belong to $K_3La_2(L\text{-}O)_2^-$ (F_w = 1029.59). The second peak group showing the highest intensity in the region 494.9−496.4 *m*/*z* with a frequency of 0.5 *m*/*z* units belongs to the double-charged species $K_2La_2(L\text{-}O)_2^{2-}$ (F_w = 990.49). The next two peak groups at lower *m*/*z* values are associated with protonated species. The signals at around 475.9−477.5 *m*/*z* can be assigned as the double-charged $(H)KLa_2(L\text{-}O)_2^{2-}$ (F_w = 952.40) species and the peaks in the range of 456.5−457.99 *m*/*z* presumably belong to the $(H)_2La_2(L\text{-}O)_2^{2-}$ (F_w = 914.30) species. The peaks in the 450.9−452.4 *m*/*z* region are the result of the fragmentation of the main complex in the gas phase ($K_2La_2(L\text{-}O)_2^{2-}\text{-}CO_2$), and species formed by the loss of a second molecule of CO_2 were also detected in the 406.9−408.4 *m*/*z* range. Species with a higher charge (3− or 4−) were not observed for either La^{3+} or the other lanthanides.

(38) Deery, M. J.; Fernandez, T.; Howarth, O. W.; Jennings K. R. *J. Chem. Soc., Dalton Trans.* **1998**, 2177.

The ESI-TOF MS spectrum obtained for the Nd^{3+} complex shows four peak groups in the 400−500 *m*/*z* region with a peak frequency of 0.5 *m*/*z* (Figure S3). The signals in this region are characteristic for the double-charged dimer structures $K_2Nd_2(L\text{-}O)_2^{2-}$, $(H)KNd_2(L\text{-}O)_2^{2-}$, and $(H)_2Nd_2(L-O)_2^{2-}$ with *m*/*z* values of 497.9−502.9 (F_w = 1001.15), 478.8−483.9 (F_w = 963.06), and 459.9−464.9 (F_w = 924.94), respectively. Similar to the La^{3+} complex, decarboxylation of the species $K_2Nd_2(L\text{-}O)_2^{2-}$ was also detected in the 450.9−455.9 *m*/*z* region. The signal of the monocharged ion $K_3Nd_2(L\text{-}O)_2^{-}$ was not found in the spectrum in this case. In the spectra of the Lu^{3+} complex, three signal groups were found which were assigned as the following species: $K_2Lu_2(L\text{-}O)_2^{2-}$ (*m*/*z* 530.96−531.95, F_w = 1062.61), $(H)KLu_2(L\text{-}O)_2^{2-}$ (*m*/*z* 511.97−512.99, F_w = 1024.52), and $(H)_2Lu_2(L\text{-}O)_2^{2-}$ (*m*/*z* 492.85−494.01, F_w = 986.42).

The results of the ESI-TOF MS studies unambiguously show that between the L-OH ligand and Ln^{3+}ions at a 1:1 metal-to-ligand ratio and a pH of around 8, dimer complexes, $Ln_2(L\text{-}O)_2^{4-}$, are preferentially formed in solution even if the concentration is about 10 times lower than in the samples used for the pH potentiometric titration experiments.

NMR Spectroscopic Studies. The relaxation rates of water protons were found to be directly proportional to the concentration of $Gd_2(L\text{-}O)_2^{4-}$ in a broad concentration range which is possible only if the composition of the Gd^{3+} complex does not change by dilution. On the other hand, the results of the ESI-TOF MS studies indicated the presence of dimer complexes even in very dilute (0.25 mM) solutions. The equilibrium data could also be described by assuming the predominance of the dimer species in solution at about pH > 7 for the La^{3+} and at pH > 4 for the Lu^{3+} complexes. These data strongly suggest that the complexes have similar dinuclear dimer structures both in solution and the solid state. So, for the interpretation of the results obtained by 1D and 2D ^1H and ^{13}C NMR spectroscopy, we assumed the existence of dimer species (e.g., $La_2(L\text{-}O)_2^{4-}$). In the interpretation of the results of earlier ^1H (1D) NMR spectroscopic studies, the dissociation of the alcoholic OH group of L-OH and the formation of dimer complexes was not taken into consideration, so the assignment of the spectra was not correct.[14]

The ^1H NMR spectrum of the deprotonated $(L\text{-}OH)^{4-}$ ligand at pD = 11.85 consists of three multiplets. A triplet of triplets (ABX pattern) of the methyne proton is at 3.81 ppm. Signals at 3.26 ppm (A) and 3.18 ppm (B) are from the AB pattern of eight chemically equivalent acetate methylene protons (*ac*AB). The signals (ABX pattern) of the four chain methylene protons are at 2.64 ppm (A) and at 2.45 ppm (B) (Figure S4a and Table S2). In the ^{13}C NMR spectrum of the ligand, there are three signals. The acetate methylene and chain carbon atoms show resonances at 61.64 ppm, the methyne carbon signal appears at 69.01 ppm, and the signal of the carbonyls at 182.36 ppm (Figure S4b).

The ^1H and ^{13}C NMR spectra of the $(L\text{-}OH)^{4-}$ ligand in the presence of equivalent amounts of La^{3+} (pD = 7.74) are much more complicated (Figure 7 and Table S2), but the line width of the proton signals do not change in a broad concentration range of 0.001−0.2 M. On the basis of these findings, we concluded that the composition of the complex formed does not change in this concentration range (there is no association or dissociation), and the dinuclear species, $La_2(L\text{-}O)_2^{4-}$, exists throughout the entire concentration range studied.

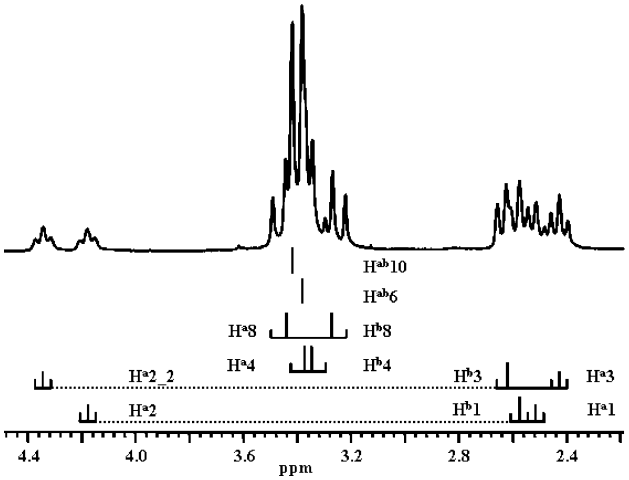

Figure 7. High-resolution ^1H NMR spectrum of the $La_2(L\text{-}O)_2^{4-}$ complex at pD 7.73, and the coupling scheme determined from the cross-peaks of the 2D COSY spectrum (Figure S8, $C_{complex}$ = 0.1 M, 298 K).

If the structure of the $La_2(L\text{-}O)_2^{4-}$ complex in solution is similar to the solid-state structure of $Nd_2(L\text{-}O)_2^{4-}$, because of the presence of the inversion center in this structure, 12 carbon signals (8 aliphatic and 4 carbonyl) and 14 proton resonances can be expected as found for $Eu_2(L\text{-}O)_2^{4-}$ at low temperatures (Figure S5). At room temperature in the ^1H NMR spectrum, only the water signal was found; the other signals were too broad to detect them. However, with the decrease of temperature to 273 K (frozen structures), 14 resonances were detectable in the ^1H NMR spectrum, but the signals were still broad (Figure S5). With the increase of the temperature, the peaks broadened, and close to the higher temperature limit (353 K), 8 peaks were observed.

The 360 MHz proton NMR spectrum of $La_2(L\text{-}O)_2^{4-}$ consists of 10 signals in the range of 2.3−4.5 ppm (Figure 7). The *J*-modulated $^{13}C\{^1H\}$ NMR spectrum shows 8 aliphatic (Figures S6 and S7) and 4 carbonyl resonances. Two carbon resonances of the *J*-modulated $^{13}C\{^1H\}$ spectrum at 73.61 and 73.48 ppm can be assigned to the C2 and C2_2 atoms, respectively. On the basis of the $^1H-^{13}C\{^1H\}$ HETCOR spectrum (Figure S7), the proton signals, H2_2 (4.36 ppm) and H2 (4.19 ppm), which integrate to one proton each, can easily be assigned to the two different methyne protons. The labeling for carbon atoms is the same as the crystallographic labels for the $K_4[Nd_2(L\text{-}O_2)]$ complex, while the labeling for protons is H for methyne and H^a and H^b for the methylene protons attached to the questionable carbon atom (Scheme 1). Six sets of methylene signals were observed for which the protons are magnetically nonequivalent as indicated by single (H) or pairs (H^a and H^b) of proton signals associated with single carbon resonances (Scheme 1). On the basis of the $^1H-^1H$ COSY experiment (Figure S8), it was easy to assign the protons of the chain methylene groups because of their coupling with the methyne (H2 and

Scheme 1. Numbering Scheme Used to Label the Proton and Carbon Atoms in the Complex Ion $La_2(L\text{-}O)_2^{4-}$

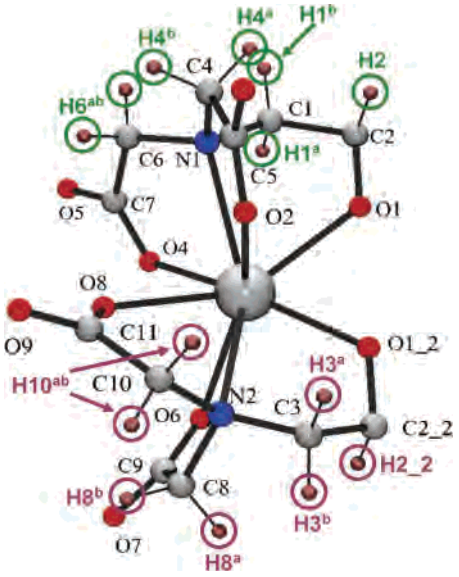

Scheme 2. Torsion Angle Between Chain Protons (a) and Dihedral Angle for the $R-CH_2-COO^-$ Fragment (b)

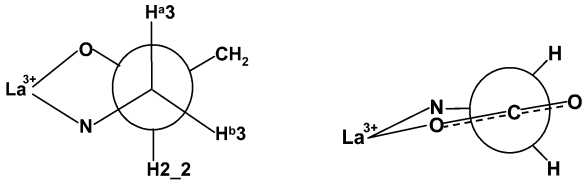

H2_2) protons. In this way, the "pseudotriplet" centered at 2.44 ppm was assigned to the H^a3 proton ($^2J_{HH}\{H^b3\} = 11.6$ and $^3J_{HH}\{H2\_2\} = 10.0$ Hz) on the C3 carbon atom with chemical shift 67.38 ppm. The torsion angle between the H^a3 and H2_2 protons on the basis of Karplus relationship is close to axial (ca. 170° with a large coupling constant) (Scheme 2a). The doublet centered at 2.65 ppm belongs to the signal of the H^b3 proton ($^2J_{HH}\{H^a3\} = 11.6$ Hz and $^3J_{HH}\{H2\_2\} \approx 1.7$ Hz) which is in the equatorial position to the H2_2 proton (ca. 50° with small coupling constant). These findings are in a good agreement with the X-ray crystallographic data of the $[Nd_2(L\text{-}O)_2]^{4-}$ complex anion, where for these angles, values of 178.9, −163.6, 59.7, and −45.2°, respectively, were found. Similarly, the signals of protons on the C1 carbon atom (66.60 ppm) were observed as a "pseudotriplet" centered at 2.53 ppm, assigned to the proton H^a1 ($^2J_{HH}\{H^b1\} = 11.6$ Hz and $^3J_{HH}\{H2\} = 10.0$ Hz, axial), and a doublet signal centered at 2.60 ppm for the proton H^b1 ($^2J_{HH}\{H^a1\} = 11.6$ Hz and $^3J_{HH}\{H2\} \approx 1.7$ Hz, equatorial). These findings are consistent with the results of selective homonuclear decoupling experiments, where the signals of H2_2 at 4.36 ppm and H2 at 4.19 ppm were irradiated and then the spectrum was recorded. The comparison of these spectra shows the coupled pair of the irradiated protons (Figures S8 and S9). The signals of H^a3 and H^a1 appear as triplets because of the large geminal and vicinal couplings with protons H2 and H2_2, respectively.

The assignment of the acetate protons was achieved with the use of through-space nOe correlation spectroscopy

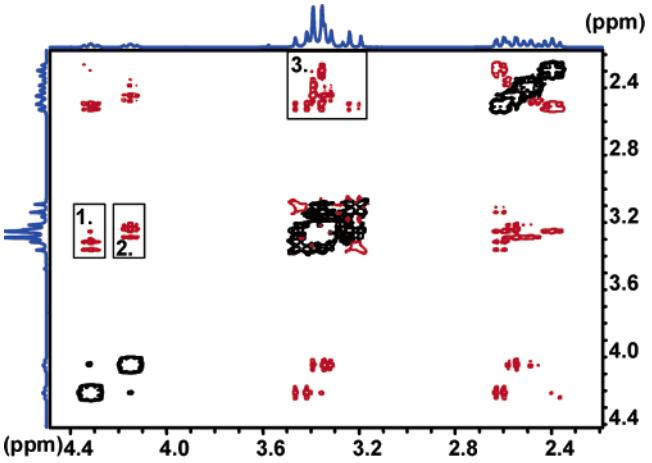

Figure 8. 2D $^1H-^1H$ NOESY spectrum of the $La_2(L\text{-}O)_2^{4-}$ complex at pD 7.73, acquired with a mixing time of 400 ms at 298 K ($C_{complex} = 0.1$ M, the most important nOe peaks needed for the assignment are boxed).

(NOESY). Figure 8 shows the 2D NOESY spectra of the complex acquired with the mixing time of 400 ms. When this quite long mixing time was used for the evaluation of the nOe effect, some residual chemical exchange peaks (detectable on the acetate proton signals) are still apparent, but the major part of the data consists of through-space nOe peaks (major and most important peaks for the correct assignment are boxed). The appearance of negative cross-peaks (box **1**) between the methyne proton H2_2 and one of the acetate protons shows a strong interaction between the spins of these protons. This is possible if these protons are on the same ligand and close to each other in space. This acetate proton is probably the H^a8 proton (Scheme 1) with a chemical shift of 3.47 ppm. However, from the $^1H-^{13}C\{^1H\}$ HETCOR spectrum (Figure S7), both the proton coupled to H^a8 and the carbon atom to which they are attached to can be easily determined. The signal at 3.27 ppm can be assigned to the H^b8 proton with geminal coupling $^2J_{HH}\{H^a8\} = 17.4$ Hz which is an exceptionally large value, while the signal at 63.15 ppm in the ^{13}C NMR spectrum can be attributed to the C8 atom. However, there is a rule supported with experimental data and quantum chemical calculations for the $R-CH_2-COO^-$ fragments predicting the variation of the $^2J_{HH}$ with the dihedral angle of the R−C bond and COO^- plane. According to the literature data, if the coupling constant is around 12 Hz, the angle is about 90°, while if it is in the range of −18 to −19 Hz, the angle is close to 0 or 180°.[39−41] The large coupling constant is the result of the coordination which stabilizes the conformation with a dihedral angle of around 180°. The coordination mode is demonstrated in Scheme 2b. Indeed, it is easy to see from the X-ray structure of the complex $Nd_2(L\text{-}O)_2^{4-}$ (Figure 1) that, for instance, the atoms N2−C8−C9−O6 are almost in the same plane.

Identically to the previously described results, the proton signal of H^a4 can be recognized from the nOe spectra because

(39) Moore, G. J.; Sillerud, L. O. *J. Magn. Reson.* **1994**, *103*, 87.
(40) Barfield, M.; Grant, D. M. *J. Am. Chem. Soc.* **1963**, *85*, 1899.
(41) Barfield, M.; Hruby, V. J.; Meraldi, J. P. *J. Am. Chem. Soc.* **1976**, *98*, 1308.

of the presence of an nOe cross-peak (box **2**, Figure 8). The signal at 3.40 ppm can be attributed to the H^a4 proton, and therefore, the coupled proton at 3.34 ppm must be H^b4 on the same C4 carbon atom with a chemical shift of 64.47 ppm. Moreover, these protons must be on the other ligand. The geminal coupling between the protons is exactly the same, and for H^a4, $^2J_{HH}\{H^b4\} = 17.4$ Hz. The remaining signals in both the ^1H and ^{13}C NMR spectra were assigned on the basis of the analysis of nOe peaks between the chain and acetate proton signals (box **3**, Figure 8). As a result, the singlet signal at 3.39 ppm and the carbon signal at 65.69 ppm are assigned to $H^{ab}10$ and C10, respectively. The H^{ab}-10 protons give nOe cross-peaks with H^a and H^b protons on the C3 carbon atom. This is only possible if the aforementioned protons are present on the same ligand. Similarly, the signals at 3.43 and 66.84 ppm in the ^{13}C NMR spectrum can be assigned to $H^{ab}6$ and C6, respectively.

Usually, important structural information can be extracted from three-bond heteronuclear couplings ($^3J_{CH}$).[42] In our case, because of the exchange processes, the signals were quite broad (10−12 Hz), and it was practically impossible to obtain useful information from these coupling constants (Figure S6). The coupling constants can be determined only for some carbonyl signals: 4.6 Hz for separate C7 and C11 carbonyl resonances. The assignment was made on the basis of 2D $^1H-^{13}C$ COLOC data set. Figure S10 shows an expansion of the carbonyl-to-acetate proton region of the 2D $^1H-^{13}C$ COLOC spectrum. According to the spectrum, the singlet peak of $H^{ab}6$ correlates with carbonyl resonance at 182.64 ppm and can be assigned to the C7 atom. The proton signal of $H^{ab}10$ correlates with carbonyl resonance at 183.18 ppm and can be assigned to carbon atom C11. The remaining carbonyl resonances at 183.65 and 183.69 ppm correlate with the AB pattern of the acetate methylene protons on the C4 and C8 carbon atoms and can be dedicated to the C9 and C5 carbon atoms, respectively.

The peaks of $H^{ab}10$ and $H^{ab}6$ protons are singlets, which may be attributed to the chemical exchange process in solution. During the chemical exchange, the H^a8 and H^b8 protons take on the identity of $H^{ab}10$ and vice versa, and similar exchanges for H^a4 and H^b4 protons with $H^{ab}6$ protons on the second ligand can also occur. This is an exchange between protons of two acetate groups attached to the same nitrogen atom. However, in the case of ligand interconversion, a similar exchange process might be present between chain protons (H^a1 to H^a3 and H^b1 to H^b3) and carbon atoms (C1 to C3). This exchange process requires the rupture of the La−alkoxy O bonds, which must be a slow process, since these bonds exhibit a long lifetime on the NMR time scale. This is in good agreement with the $^{13}C-^{13}C$ EXSY spectra measured with various mixing times. The methylene region of the $^{13}C-^{13}C$ EXSY spectrum measured with a mixing time of 200 ms is shown in Figure 9. Cross-peaks **1** and **2** in Figure 9 can be assigned to the exchange of acetate (C4−C6 and C8−C10) methylene carbon atoms. The presence of exchange peaks on the acetate and the absence of exchange

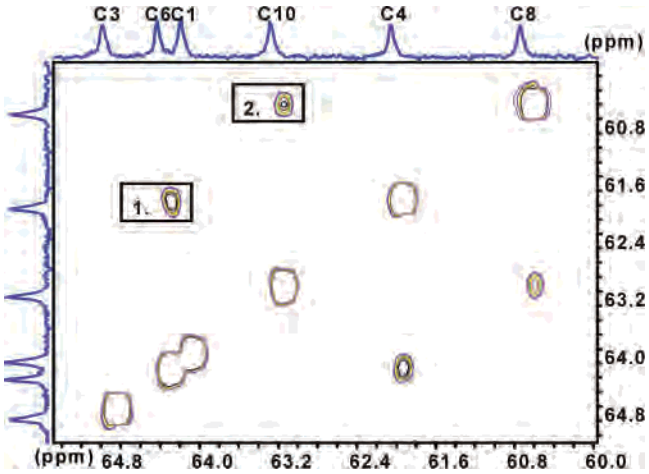

Figure 9. Methylene part of the 2D $^{13}C-^{13}C$ EXSY spectrum of the $La_2(L\text{-}O)_2^{4-}$ complex at pD 7.73, acquired with a mixing time of 200 ms at 298 K ($C_{complex} = 0.1$ M, the exchange peaks are boxed).

between the chain methylene (C1 and C3) carbon atoms are in good agreement with our speculations. The carbonyl region of the $^{13}C-^{13}C$ EXSY spectra measured with a mixing time of 600 ms is presented in the Figure S11. The exchange peaks marked with boxes **1** and **2** result from the exchange process between carbonyls C5−C7 and C9−C11, but cross-peak **3** can be the result of the ligand interconversion process (exchange C7−C11) which occurs with a slower rate.

^1H NMR spectroscopy was used to monitor the temperature-dependent behavior of the $La_2(L\text{-}O)_2^{4-}$ complex anion in D_2O over the range of 273−353 K (Figure S12). With the increase of temperature, the signals broadened indicating the increase of the exchange rates at higher temperatures. The signal of H2_2 at 333 K in the ^1H NMR spectrum could not be detected, but by 2D $^1H-^1H$ COSY, it was found to overlap the water signal (cross-peak with water in Figure S13). At 353 K, the signal of H2 behaves similarly. Surprisingly, even at the highest temperature, there was no coalescence of the signals, and the AB multiplet pattern was observed both for the chain and acetate methylene resonances.

Conclusions

The presence of the alcoholic OH group in the aminopolycarboxylate ligand H_4L-OH significantly changes its complexation properties in comparison with those of the analogous H_4dpta or H_4edta.The stability constants of the lanthanide(III) complexes formed with the heptadentate $(L\text{-}OH)^{4-}$ are somewhat lower than those of the hexadentate $(dpta)^{4-}$ probably because of the lower basicities of the nitrogen atoms of $(L\text{-}OH)^{4-}$. However, the coordination of the two iminodiacetate groups of the ligand leads to strong interactions between the alcoholic oxygen and the Ln^{3+} ion, and the alcoholic OH group dissociates at unexpectedly low pH values. The pH range of the dissociation shifts to more acidic regions with the decrease of the size of the Ln^{3+} ion, which indicates the electrostatic nature of the metal−ligand interactions.

The coordinated heptadentate $(L\text{-}O)^{5-}$ ligand, containing an alkoxo oxygen, shows a strong propensity to form

(42) Thomas, W. A. *Prog. Nucl. Magn. Reson. Spectrosc.* **1997**, *30*, 183.

dinuclear dimer complex anions, $Ln_2(L-O)_2^{4-}$, both in solution and solid state. In the dinuclear dimers the ligands are coordinated to both Ln^{3+} ions with an iminodiacetate group, and the alkoxo oxygens are in bridging positions. The coordination number of the Ln^{3+} ions is 9 in the complexes of the lighter elements, with one water molecule per Ln(III) ion in the inner sphere (e.g., the solid $K_4[Nd_2(L\text{-}O)_2(H_2O)_2]\cdot 14H_2O$). The structure of the dinuclear dimers of the heavier elements is highly stable with 8 coordinated Ln^{3+} ions (Ho and Lu complexes).[20] The probable absence of the water molecule in the inner sphere of the Gd^{3+} complex is indicated by the unusually low relaxivity value of $Gd_2(L\text{-}O)_2^{4-}$, which also shows the formation of dimer species with the heptadentate ligand $(L\text{-}O)^{5-}$.

The geometries of the dimer complexes of the lighter and heavier lanthanides are different. In the complexes of the heavier elements in the solid state, there is a symmetry plane,[20] while in the Nd^{3+} dimer, the only symmetry element is a center of symmetry.

The solution structure of the $La_2(L\text{-}O)_2^{4-}$ complex studied by 1D and 2D NMR spectroscopy is similar to the solid-state structure of the $Nd_2(L\text{-}O)_2^{4-}$ anion, obtained by X-ray diffraction studies.

Acknowledgment. Financial support from the Hungarian Scientific Research Found (OTKA T 043365 and T 038364) are gratefully acknowledged. A.B. is grateful for the Hungarian Academy of Sciences for István Széchenyi Fellowhip. The authors are indebted to Dr. Sándor Kéki and Dr. János Török for their help in the collection of ESI-TOF MS data and to Judit Vanka and Béla Rózsa for their assistance in the collection of pH potentiometric titration data.

Supporting Information Available: Tables of additional crystallographic and refinement parameters in CIF format, geometry data of hydrogen bonds in $K_4[Nd_2(L\text{-}O)_2(H_2O)_2]\cdot 14H_2O$, ^1H NMR chemical shifts and coupling constants for the $L\text{-}OH^{4-}$ ligand and $La_2(L-O)_2^{4-}$ complex (Tables S1 and S2), temperature dependence of the relaxivity (r_1) of $Gd_2(L\text{-}O)_2^{4-}$ complex (Figure S1), proton relaxation rates versus total concentration of $Gd_2(L\text{-}O)_2^{4-}$ (Figure S2), ESI-TOF MS spectrum of the solution containing equimolar amounts of Nd^{3+} and L-OH (0.25 mM) (Figure S3), ^1H and ^{13}C NMR spectra of the free ligand (Figure S4), temperature dependence of the ^1H NMR spectra of $Eu_2(L\text{-}O)_2^{4-}$ (Figure S5), $^{13}C\{^1H\}$ *J*-modulated and proton-coupled ^{13}C NMR spectrum of the $La_2(L\text{-}O)_2^{4-}$ complex (Figure S6), $^1H-^{13}C\{H\}$ HETCOR and $^1H-^1H$ COSY spectra of the $La_2(L\text{-}O)_2^{4-}$ anion (Figures S7 and S8, respectively), selective decoupling experiment for the $La_2(L\text{-}O)_2^{4-}$ complex (Figure S9), carbonyl-to-acetate proton region of the 2D $^1H-^{13}C$ COLOC spectrum of the $La_2(L\text{-}O)_2^{4-}$ anion at pD 7.73 optimized for 4.6 Hz long-range couplings (Figure S10), carbonyl region of the 2D $^{13}C-^{13}C$ EXSY spectrum of the $La_2(L\text{-}O)_2^{4-}$ complex (Figure S11), temperature dependence of the ^1H NMR spectra of the $La_2(L\text{-}O)_2^{4-}$ complex (Figure S12), and the 2D $^1H-^1H$ COSY spectrum of the $La_2(L\text{-}O)_2^{4-}$ complex at 333 K and 500 MHz (Figure S13). This material is available free of charge via the Internet at http://pubs.acs.org.

IC0517321